SICE Annual Conference 2010
August 18-21, 2010, The Grand Hotel, Taipei, Taiwan

Penalty Kick of a Humanoid Robot by a Neural-Network-Based Active Embedded Vision System

Chih-Lyang Hwang, Nien-Wen Lu, Tim-Chia Hsu and Chun-Hao Huang

Department of Electrical Engineering, Tamkang University, 25137 Taiwan, R.O.C.

Abstract ---This paper realizes the humanoid robotic system to execute the penalty kick (PK) of the soccer game. The proposed system includes the following three subsystems: a humanoid robot (HR) with 22 degree-of-freedom, a soccer with different colors, and a soccer gate. In the beginning, the HR scans the soccer field to find the gate and the soccer, which are randomly distributed in a specific region in the front of the gate. If a command for the PK of the soccer with specific color is assigned, the HR will be navigated by an active embedded vision system (AEVS). After the HR reaches a planned position and posture, the PK of the HR will be executed. Two key important techniques are developed and integrated into the corresponding task. One is the modeling using multilayer neural network (MNN) for different view angles, the other is the visual navigation strategy for the PK of the HR. In addition, the error sensitivities in the pan and tilt directions of these four visible regions are analyzed and compared. The proposed strategy of the visual navigation includes the following two parts: (i) the switched visible regions are designed to navigate the HR to the planned position, and (ii) the posture revision of the HR in the neighborhood of the soccer in order to execute the PK. Finally, a sequence of experiments for the PK of the HR confirm the effectiveness and efficiency of the propose methodology.

Keywords: Humanoid robot, Penalty kick, Image processing for localization, Modeling using multilayer neural network, Strategy for visual navigation, Posture revision.

I. Introduction

There are many researches about autonomous humanoid robot [1]-[13]. Their corresponding topics are expressed as follows. In recent years, Loffler et al. [1] discussed sensors and control concept of a biped robot. A known forward operation for a specific task combined with the sensory reflex control for a humanoid robot was developed by Huang and Nakamura [2]. In addition, a stepping over obstacles with humanoid robot was discussed by Guan et al. [3]. It merely discussed the static balance. Harada et al [4] discussed a real-time planning of humanoid robot's gait for force-controlled manipulation. Neo et al. [5] discussed the whole-body motion generation integrating operator's intention and robot's autonomy in controlling humanoid robots. A new active visual for humanoid robot was discussed by Xu et al. [6]. Arechavaleta et al. [7] discussed an optimality principle governing human walking. Montesano et al. [8] demonstrated successful learning in the real world by having a humanoid robot interacting with objects. Gait synthesis and sensory control of the stair climbing for a humanoid robot was discussed by Fu and Chen [9]. In addition, Kanda *et* al. [10] investigated the interactions between human and humanoid robots: Robovie and ASIMO. Yoshida et al. [11] planned a 3-D collision-free dynamic robotic motion through iterative reshaping. Recently, **the paper [12] presented three feedback controllers that achieve an asymptotically stable, periodic, and fast walking gait for a 3-D bipedal robot consisting of a torso, revolute knees, and passive point feet. According to the above analysis, h**umanoid robots are expected to take an important role in assisting activity in human daily environments owing to their flexibility and friendly appearance.

In this paper, the PK of the soccer for the HR using an active embedded vision system (AEVS) is developed. At first, the AEVS will search the soccer field, when the soccer of assigned color (e.g., green or blue color) is found, the system transforms the color image into a binary image by thresholding technique so that the computation time and storage requirement are reduced. However, the binary image still has a little noise, the noise removal of two-steps procedure is suggested to remove (or eliminate) them. The first step uses a median filter to reduce most of the noise; the second step is to segment the binary image based on the information of the area and circumference of the image. In summary, the proposed noise removal is effective and efficient. After the noise removal, some destructions in the binary image occur and the central position of the image of the soccer is not at its real central position. Therefore, the image restoration is required to hold the central position of the soccer after the previous image processing. Finally, the area and central position of the specific soccer on the image plane coordinate are obtained.

It is known that a relation between the image plane coordinate and the world coordinate is highly nonlinear. It is also known that a neural network is suitable for the (especially nonlinear) function approximation (or modeling) via various learning algorithms. However, a multilayer neural network (MNN) with LMBP learning algorithm is applied to build the transformation between the image plane coordinate and the world coordinate. The main features of the LMBP learning algorithm are that it possesses the fastest convergence with acceptable learning error as compared with other learning algorithms, and that it has poor performance as the number of the input for the MNN is large. Fortunately, only two inputs for the modeling are assumed in this paper. Different view angles of the AEVS are considered to obtain different visible regions such that the connection of these regions becomes an effective visual navigation for the HR.

As one knows, the ideal posture of the HR for the PK must contain the following two factors: one is that the standing position of the HR must in the line and same orientation between the virtue target point (e.g., 1/4 distance of the width of the gate from its left or right column) and the assigned soccer, the other is to obtain

the suitable distance between the HR and the assigned soccer. Based on the above two requirements, the posture revision is designed. It includes the following two steps: (i) the revision of the orientation of the HR, and (ii) the revision of the position of the HR. After the posture revision, the HR will be in the neighborhood of the ideal posture for the PK. Finally, the smallest visual window is employed to modify the fine adjustment of the HR to obtain a perfect task of the PK.

The organization of this paper is described as follows. In the next section, the experimental setup and task description are given. In section 3, the image processing for localization of the soccer is addressed. In section 4, the modeling for four view angles via the multilayer neural network (MNN) with the LMBP learning algorithm is constructed. In addition, the error sensitivities in the pan and tilt directions of these four visible regions are analyzed and compared. In section 5, the strategy for the visual navigation of the HR, including the switched visible regions and the posture revision, is designed. In section 6, the experimental results and discussions are presented. Finally, the conclusions are given in section 7.

II. Experimental Setup and Task Description

A. Experimental Setup

The photograph of the HR is depicted in the Fig. 1(a), which possesses 22 degree-of-freedom (DOF) with the weight of 5 kg and the height of 50 *cm*. The specifications of the HR are described as follows: 6 DOF for each leg, 4 DOF for each arm, 1 DOF for the body (or 3 DOF for the body including 2 DOF common with two legs), and 1 DOF for the head. The corresponding DOF is expressed in Fig. 1(b). The servo motors are the Model No. of AX-12, RX-28, and RX-64 from Robotis Co. Based on the weight and torque of servomotor and the required torque for the motion of HR, the arm and head, leg, and knee of the HR respectively use the model AX-12, RX-28 and RX-64. One of dominant feature of the servomotor from Robotis Co. is its command by the peripheries of RS-485 and TTL UART, which is different from the PWM for the other servomotor.

The embedded system RB-100 for the sensor fusion and the execution of the assigned task are described as follows: dimension 96x56 mm, weight 40g, CPU DM&P Vortex86DX, 256MB DDR2, power consumption +5V @400mA, input DC voltage 6~24V, and operating system: DOS, Windows 98/ME, Windows XP/ XP Embedded, Windows Embedded CE, and Windows Embedded Standard Linux. It also contains four kind of UART: RS-232, RS-485, TTL full duplex, and TTL half duplex. An integrated circuit (see Fig. 1(c)) is also designed for the reduction of connection wire. The proposed HR also can execute the fuzzy decentralized balance control. However, it is not main topic of this paper; the details are omitted. We also design a human-interface for the operation of the HR (see Fig. 2), which can give position and velocity commands for every motor. The command can simultaneously or sequentially drive a set of specific motors.

The proposed active embedded vision system (AEVS) includes a digital signal processor of TMS320C6713 and a camera modular of VM480. The important specifications of the TMS320C6713 are floating point type, 32M Byte of SDRAM, Code Builder software, and the clock speed of 300MHz. Its total area is 55x45mm, which is suitable for the proposed HR. The camera modular includes four kinds of resolution: 60x80, 120x160, 240x320, and 480x640. The default format of the color space is $YUV=4:2:2$. One limitation for this camera modular is that the focus length is fixed and only adjusted by manual not by a software.

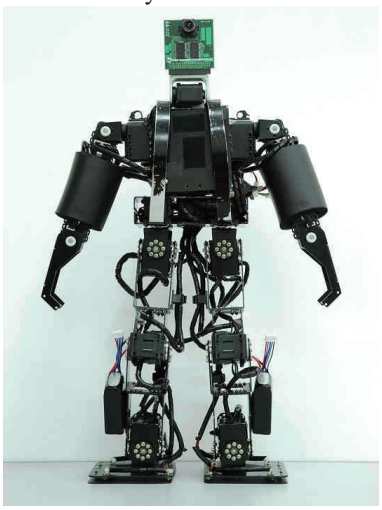

(a) Photograph.

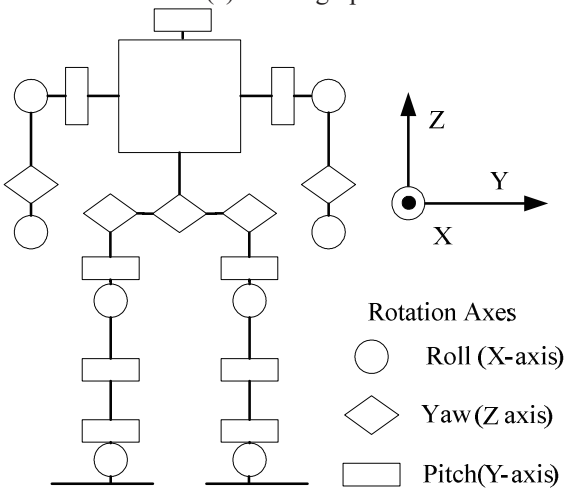

(b)DOF of HR.

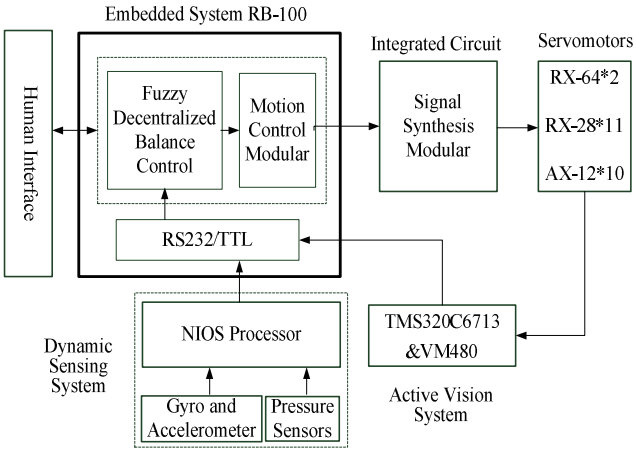

(c) Block diagram.

Fig. 1. Architecture of an HR.

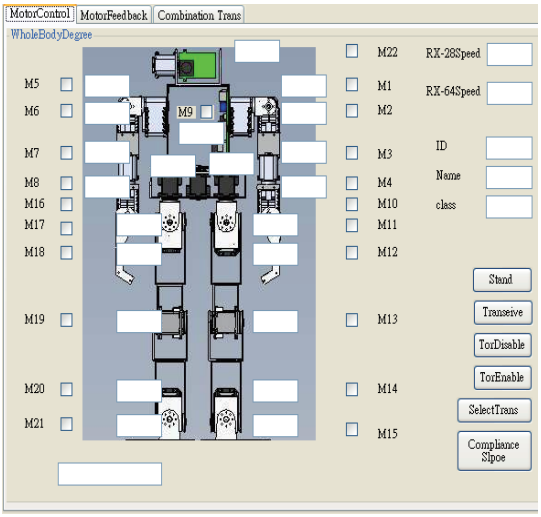

Fig. 2 A human-interface for the operation of an HR.

B. Task Description

First, the HR scans the soccer field to find the gate and the soccer, which are randomly distributed in a specific region in the front of the gate. If a command for the PK of the soccer with specific color is assigned, the HR will be navigated by an active embedded vision system (AEVS). After the HR reaches a planned position and posture, the PK of the HR will be executed.

III. Image Processing for Localization

In the task of the PK, the accuracy of the image localization is the most important factor. A successful image processing can result in an accurate localization. Hence, the flow chart of the image processing for the localization is addressed in Fig. 3, including the following five parts: image inquiry, binary image, noise removal, image restoration, and image representation.

A. Image Inquiry

For simplifying the computation, the source image with the resolution of 240x320 is used for the localization of the soccer. Because the default format of the TMS32C6317 can be YUV, where Y represents the luminance component, and U,V are chrominance components, no conversion of color space is required. After the inquiry of the source image (e.g., Figs. 4(a) and (c)), the binary processing of the corresponding source image is obtained by suitable thresholding values for different colors of the soccer.

B. Binary Image

In this paper, a double thresholding technique is applied to the component of U and V such that a binary image is obtained. The corresponding relation is

$$D(I_x,I_y)=\begin{cases}1, & \text{if } T_{b2}\ge f(I_x,I_y)\ge T_{b1}\\ 0, & \text{otherwise}\end{cases} \quad (1)$$

where $f(I_x,I_y)$ denotes the values of U and V on the image plane (I_x,I_y), $D(I_x,I_y)=1$ stands for the white pixels, and $D(I_x,I_y)=0$ stands for the black pixels. The purpose of binary processing is to reduce the storage amount as well as the computation load. The values of T_{b1} and T_{b2} are less sensitive to lighting conditions because the Y component is not considered for the binary operation. Because the background is a little bit to be red color, the green and blue soccer are chosen for the easy segmentation from the ground such that the accuracy of the localization via image processing is increased. After investigation, the suitable threshold ranges for the green soccer and the blue soccer are $[U_{min},U_{max}]=[80,115]$, $[V_{min},V_{max}]=[40,100]$, and $[U_{min},U_{max}]=[180,255]$, $[V_{min},V_{max}]=[30,90]$, respectively. The binary images are respectively shown in Figs. 4(b) and (d).

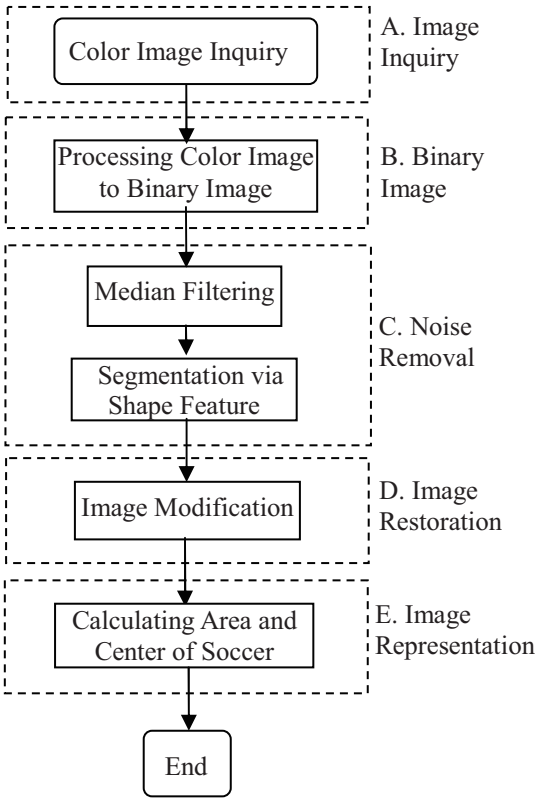

Fig. 3. Flow chart of image processing.

C. Noise Removal

There still have a little noise (i.e., black pepper, white salt, and thin line) in the binary images (e.g., Figs. 4(b) and (d)). Noise removal of this paper includes the following two procedures: (i) A medial filter is first applied to attenuate the high frequency noise. The corresponding image is shown in Fig. 5(a). The further use of medial filter must sacrifice the area of the soccer in order to reduce more the high frequency component of the binary image (e.g., the noise in the top left of Fig. 5). In this situation, the estimation errors of the area and the central position of the soccer occur. In addition, the median filter is time-consuming. It had better not to use too many times of the median filter. (ii) Under the above analysis, the shape of the soccer is applied to reduce the remained noise. The segmentation via shape feature depends on the area and circumference (i.e., $R_{shape}=4\pi\times area/circumference^2$).

In summary, if the image is exactly a circle, $R_{shape}=1$. Based on this methodology, the corresponding

result of Fig. 5(a) is shown in Fig. 5(b), which is much better than that of Fig. 4(b) or Fig. 5(a). Similarly, the noise removal of Fig. 4(d) can be obtained. For simplicity, it is omitted.

(a) Source image of green soccer.

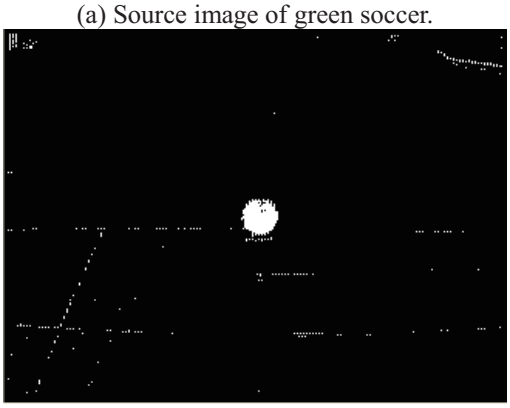

(b) Binary image of green soccer.

(c) Source image of blue soccer.

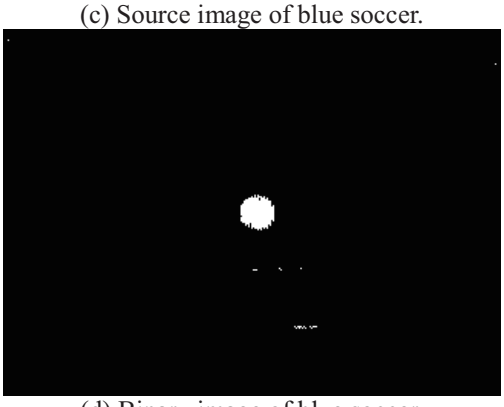

(d) Binary image of blue soccer.

Fig. 4. The image processing for the soccer.

D. Image Restoration

After the noise removal, the shape of the image for the soccer has some distortions (e.g., a notch feature in the Fig. 5(b)). This phenomenon can cause a poor estimation of the area and then the central position of the soccer. Therefore, before calculating the area and central position of the soccer, the image restoration is considered to restore its original shape in the image plane.

The procedures for the image restoration (or modification) are described as follows:

(i) Find the longest row and column axes.

(ii)Let the half position of the longest column be the symmetrical axis, and then do the logical operation OR for the opposite position of each column.

(iii) Similarly, let the half position of the longest row be the symmetrical axis, and then do the logical operation OR for the opposite position of each row (see Fig. 6).

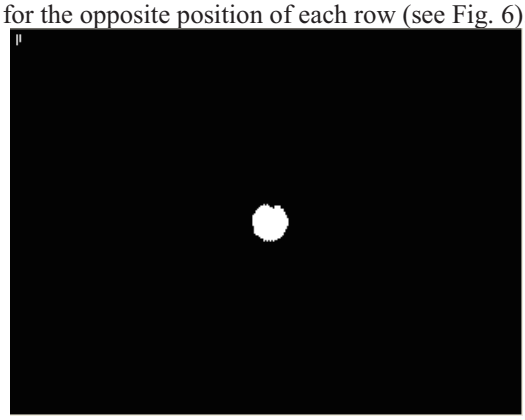

(a) Median filtering of green soccer.

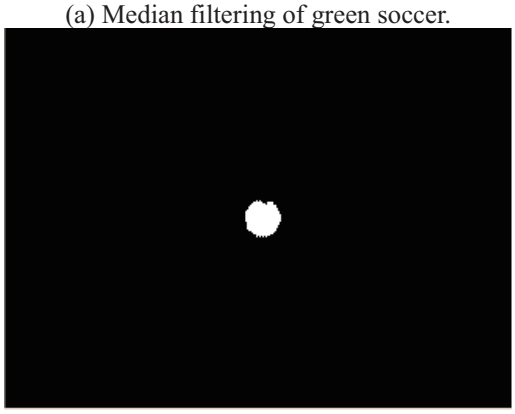

(b) Segmentation of green soccer by the feature R_{shape}.

Fig. 5. Image processing for noise removal.

E. Image Representation

The central position of the soccer can be calculated as follows:

$$\bar{I}_x = \sum_{(I_x,I_y)\in\Omega} \sum I_x / A,\ \ \bar{I}_y = \sum_{(I_x,I_y)\in\Omega} \sum I_y / A \qquad (2)$$

where $(\bar{I}_x, \bar{I}_y)$ denotes the center of the area A of the desired image feature Ω.

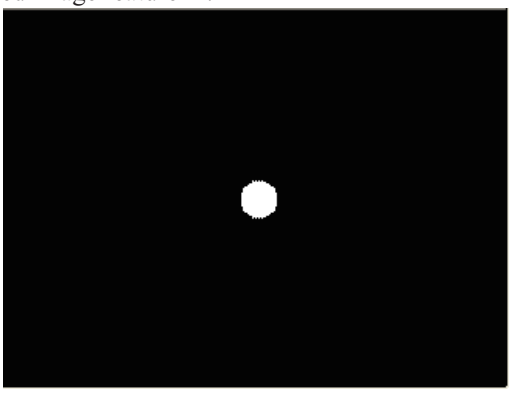

Fig.6. Image restoration via image modification.

Ⅳ. Neural Network Modeling of AEVS

A. *Multilayer Neural Network*

Figure 7 displays a relation between the image plane coordinate $A_i \sim F_i$ and the world coordinate $A_w \sim F_w$, which is highly nonlinear. It is also known that a neural network is suitable for the (especially nonlinear) function approximation (or modeling) via various learning algorithms, e.g., Conjugate Gradient Back Propagation algorithm, Levenberg Marquardt Back Propagation (LMBP) algorithm. In this situation, a multilayer neural network (MNN) with LMBP learning algorithm is applied to set up the transformation between the world coordinate and the image plane coordinate. The main features of the LMBP learning algorithm are that it possesses the fastest convergence with acceptable learning error as compared with other learning algorithms, and that it is poor as the number of the input for the MNN is large. Fortunately, only two inputs for the modeling of the proposed system.

Figure 8 shows the corresponding data for four visible regions for the modeling. The proposed architecture of MNN is shown in Fig. 9, which has the input $\mathbf{P}=\begin{bmatrix} I_x & I_y \end{bmatrix}^T$, the output $\mathbf{a}^2=\begin{bmatrix} X_w & Y_w \end{bmatrix}^T$, the number of hidden layer weights 30, $f_i^1(n_i^1)=\left(1-e^{-n_i^1}\right)\Big/\left(1+e^{-n_i^1}\right)$, $i=1,2,...,30$, and $f_j^2(n_j^2)=n_j^2, j=1,2.$ The upper-script of the symbol in Fig. 9 denotes the variable of the corresponding layer.

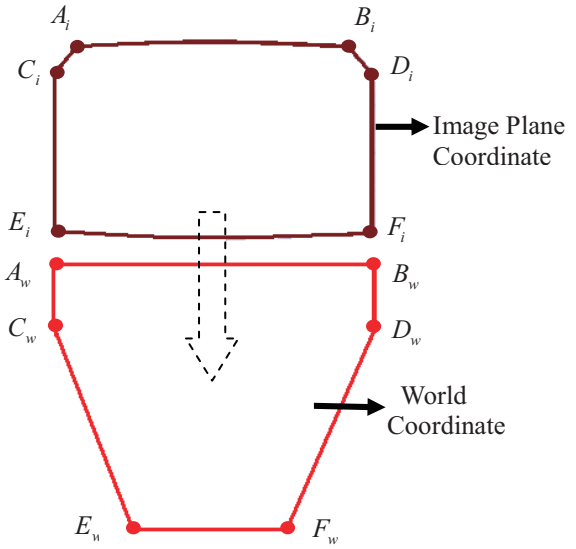

Fig. 7. The relation between the image plane and the world coordinates for $\theta=30^\circ$.

B. *Error Analysis*

After an effective learning of the MNN in Fig. 9, the error sensitivities of four visible regions are shown in Figs. 10-13. Four visible regions are respectively partitioned into 8, 6, 6, and 4 sub-regions. The numbers in every sub-region (i.e., $(e_1, \pm e_2, \pm e_3, e_4)$) represents the error (unit: *cm*) of the nominal condition, the error caused by every increment or decrement of 1 degree and in the tilt direction, the error caused by every increment or decrement of 1*cm* in the Z-axis (or height of the HR), and the average error between 1 and 5 degree of the pan direction, respectively. From Figs. 10-13, the important observations are summarized as follows: (i) After an effective modeling via MNN with LMBP algorithm, the error is approximately equal to the resolution of corresponding visible region with respect to the image pixel. (ii) The error sensitivity in the tilt direction is larger than that in the pan direction. (iii) The absolute error, the sensitivities in the tilt direction, Z-axis and the pan direction of the smallest visible region are respectively about 0.14, 0.27, 0.14, and 0.09 *cm*, which are good enough for the PK of the HR.

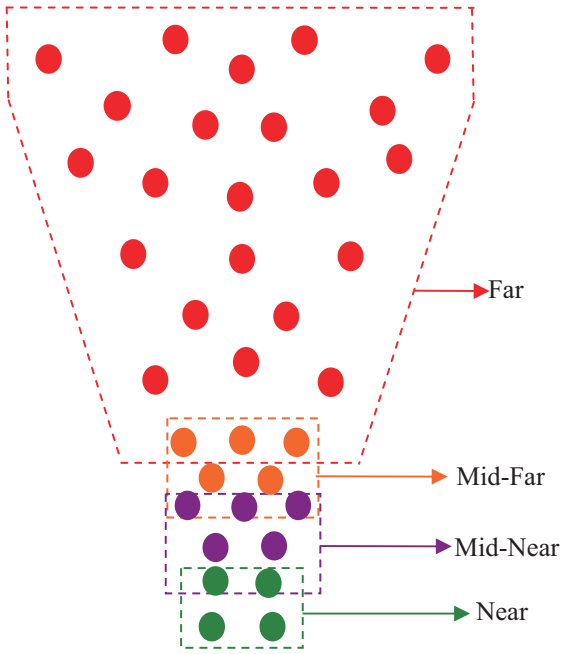

Fig. 8. Inquiry of training data.

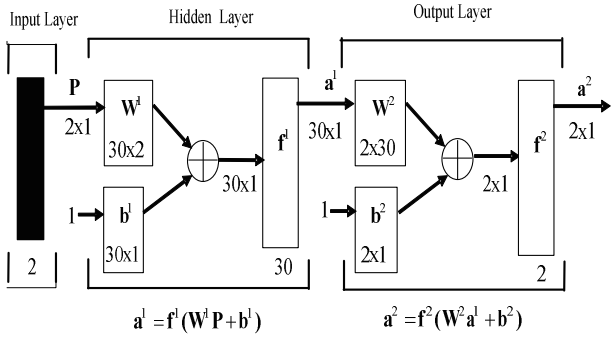

Fig. 9. Architecture of MNN.

Ⅴ. Navigation for the PK of an HR

A. *Calculation of the Posture of an HR*

After four transformations between the image plane coordinate and the world coordinate through the MNN modeling, the calculation of the posture of the HR is described as follows:

$$D=\sqrt{\left(X_{AEVS}-X_{soccer}\right)^2+\left(Y_{AEVS}-Y_{soccer}\right)^2} \quad (3)$$

$$\phi=\sin^{-1}\left(D_x/D\right) \quad (4)$$

where $\left(X_{soccer}, Y_{soccer}\right)$ and $\left(X_{AEVS}, Y_{AEVS}\right)$ denote the world coordinate of the soccer and the AEVS (or HR), $D_x=X_{AEVS}-X_{soccer}$ denotes the x component of the

distance D, ϕ is the orientation of the soccer with respect to the HR.

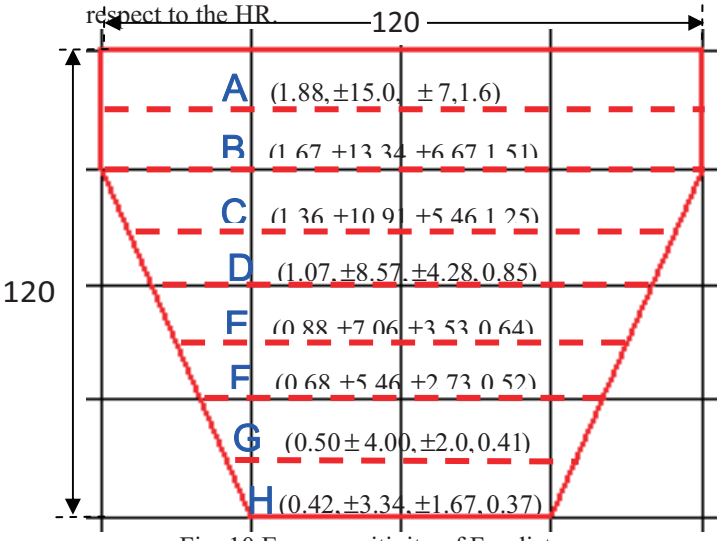

Fig. 10.Error sensitivity of Far distance.

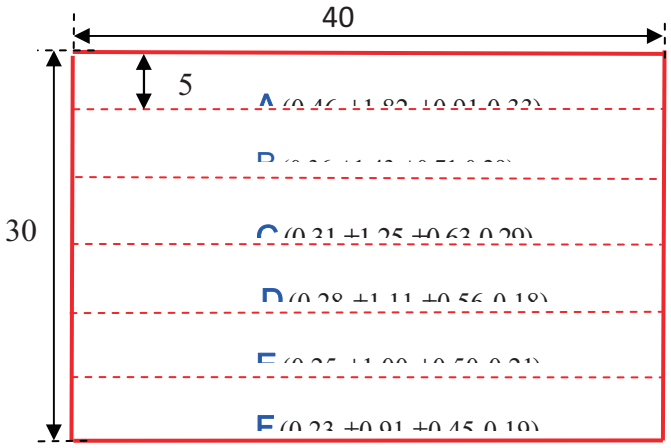

Fig. 11. Error sensitivity of Mid-Far distance.

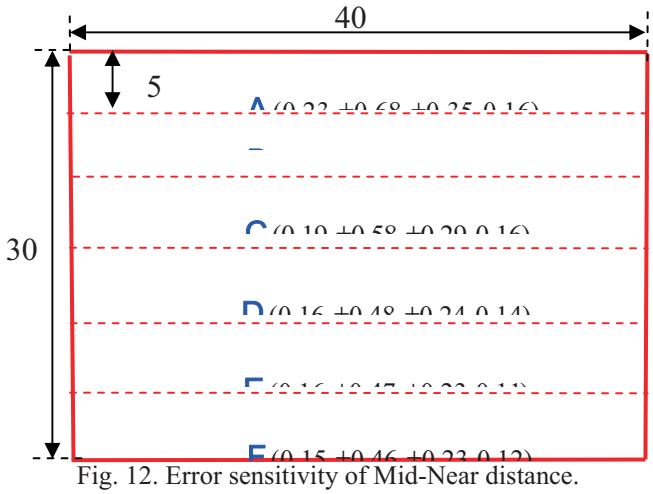

Fig. 12. Error sensitivity of Mid-Near distance.

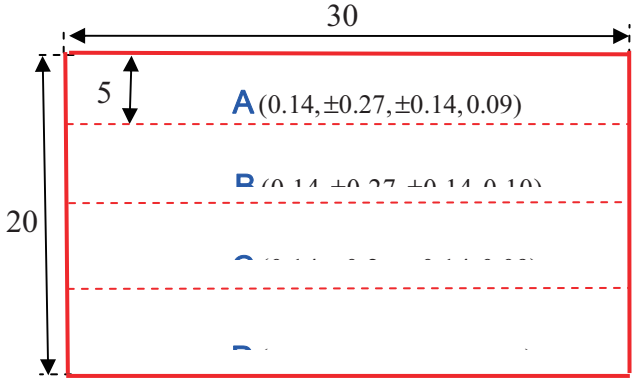

Fig. 13. Error sensitivity of Near distance.

If $D_x > 0$, then the HR must turn the angle ϕ in the clockwise (CW) direction to exactly face the soccer. On the contrary, the HR must turn the angle ϕ in the counter clockwise (CCW) direction to exactly face the soccer as $D_x < 0$. Then $D_x = 0$, indicates that the soccer is on the Y-axis, i.e., no revision of the orientation for the HR is required. After the calculation of the posture of the soccer with respect to the HR, the adjustment of the orientation is first made. Then let the HR walk the planned distance of $D_p = D - D_\delta$, where D_δ is the distance for the manipulation of the PK. In this paper, $D_\delta = 10cm$. The corresponding navigation of the HR to reach the planned position is shown in Fig. 14. Figure 15 depicts the navigation of the HR through the connection of four visible regions with suitable switching points. The symbols of R_f, R_{mf}, R_{mn}, and R_n in Fig. 15 denote respectively the Far, Mid-Far, Mid-Near, and Near distances between the soccer and the HR. Based on the result of Fig. 8, $60 \le R_f \le 180$, $40 \le R_{mf} \le 70$, $15 \le R_{mn} \le 45$, and $0 \le R_n \le 20cm$. After the reach of the planned position for the HR, the "Far"distance of the AEVS is employed to search the virtue target point in Fig. 16 and then make the necessary adjustment of the orientation of the HR (i.e., ϕ in Fig.16) to face the virtue target point. It should be noted that the localization of the virtue target point needs the search of two columns of the gate. If the HR is not consistent with the known orientation T_o in the Fig.17, it is first revised. Then the revision of position is made to execute the PK. The detail can be found in the next subsection.

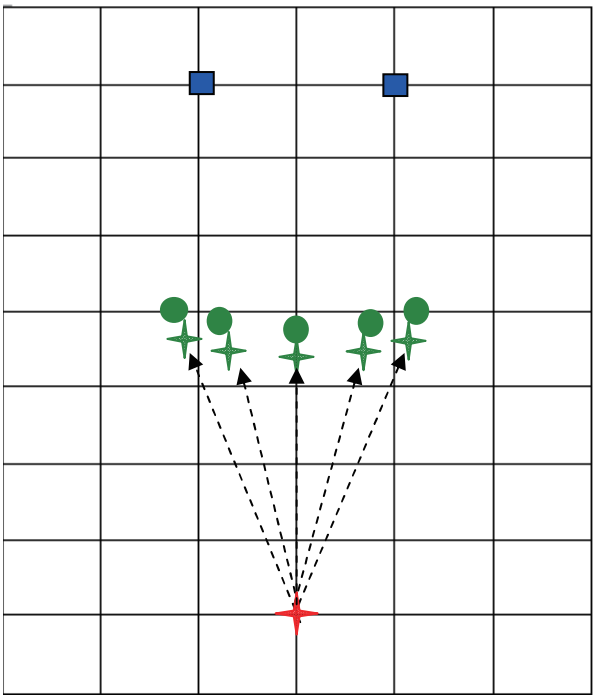

Fig. 14. The navigation of an HR to reach the planned position.

B. The Posture Revision of an HR for the PK

After the movement to the position Z, which is ideal to be the planned position, the more accurate posture is required for the PK. The result of the posture revision is designed as shown in Fig. 17, which possesses the orientation of the HR is the same as that connected between the HR and the virtue target point. The strategy of the posture revision is depicted in Fig. 18. The original orientation of the HR is in the direction of $\overrightarrow{ZX}$. It is then revised as the direction of $\overrightarrow{YX}$ based on the following equation:

$$\theta_{\overrightarrow{YZ}} = \sin^{-1}\left(2\sqrt{s\left(s-\overline{XY}\right)\left(s-\overline{XZ}\right)\left(s-\overline{YZ}\right)}\Big/\left(\overline{XY}\cdot\overline{XZ}\right)\right) \quad (5)$$

where $s = \left(\overline{XY}+\overline{XZ}+\overline{YZ}\right)/2$ .After the revision of the orientation, the position is revised as from the position Z To the position Y'. After the reach of the position Y', the HR must move a little leftward for the reason that the PK using the right foot as the soccer is on the left hand side of the initial posture of the HR. On the contrary, as the soccer is initially on the right hand side of the HR, it must move a little leftward for the PK using the right foot.

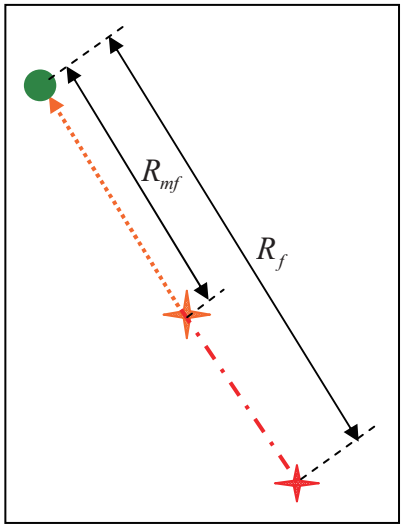

(a) Far → Middle Far distance.

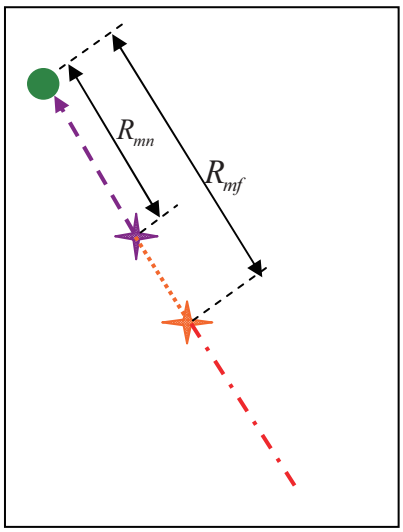

(b) Middle Far →Middle Near.

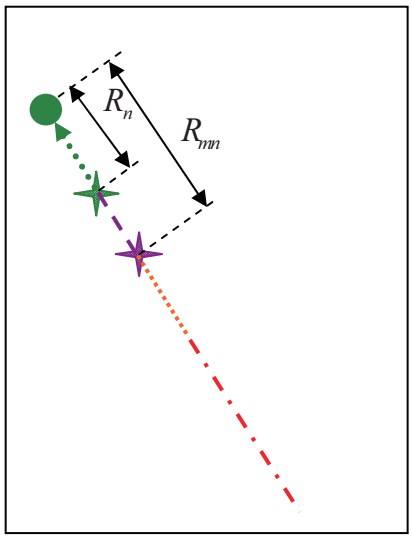

(c) Middle Near → Near.

Fig.15. Suitable switching points of four visible regions to form an AEVS.

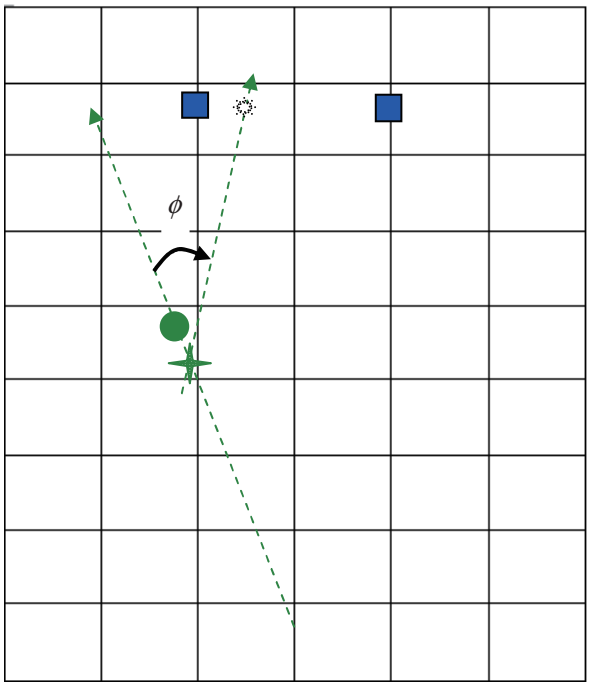

Fig. 16. The search of virtue target point and the adjustment of the orientation of the HR.

VI. Experiment Results and Discussions

Because the maximum coordinates error of experimental result by localization is only one pixel that the maximum localization error is smaller than 1.88*cm*. The higher resolution of the image is used for the localization, the better localization is obtained. However, the computation time is also increased. The computation times of the median filter, the image segmentation via shape feature, the image restoration, and neural network modeling for the 240x320 image are 43×10^{-6}s , 4×10^{-6}s, 43×10^{-6}s and 0.5×10^{-6}s, respectively. Then

the total processing time is 1.2079*s*. According to the experiment, the total processing time for the resolution 640X480 is longer than three seconds. Therefore it seems inappropriate for the task of the PK of the HR.

Finally, the corresponding experimental result for the PK of the HR is shown in Fig. 19. In this experiment, the initial posture of the HR and the soccer are respectively $(x_0, y_0, \theta_0)\big|_{HR} = (0, 0, 0^\circ)$ and $(x_0, y_0, \theta_0)\big|_{soccer} = (-43, 82, 27^\circ)$. The width of the gate and the diameter of the soccer are 60 and 8 *cm*, respectively. The total process time is about 210 second.

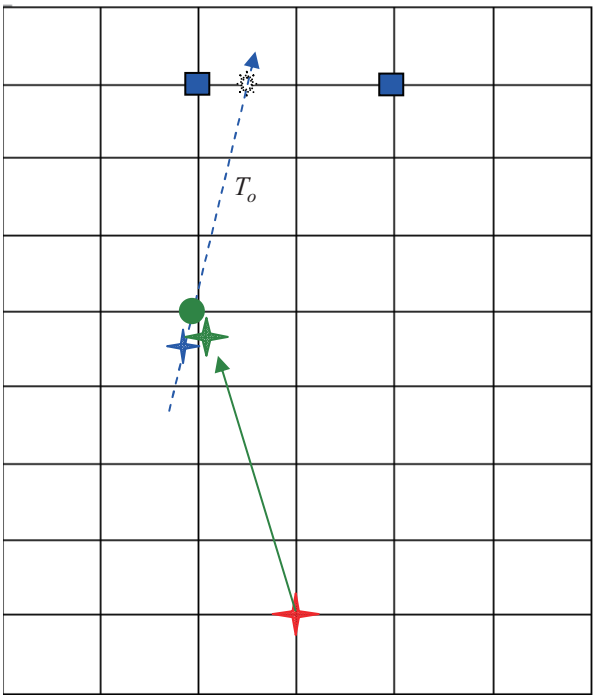

Fig. 17. The strategy of PK for an HR.

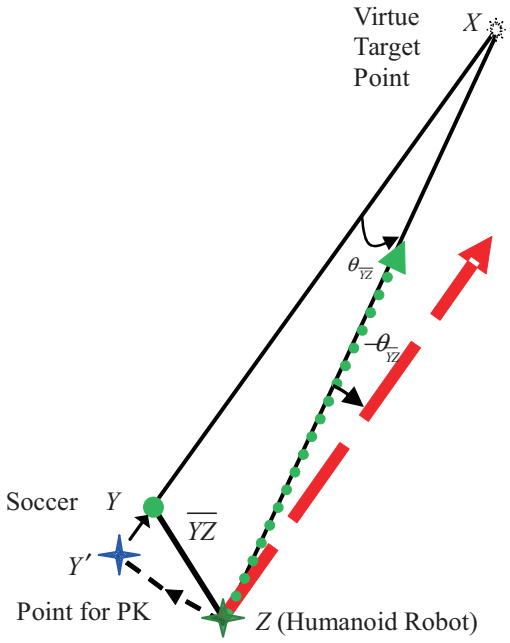

Fig. 18. The posture revision of PK.

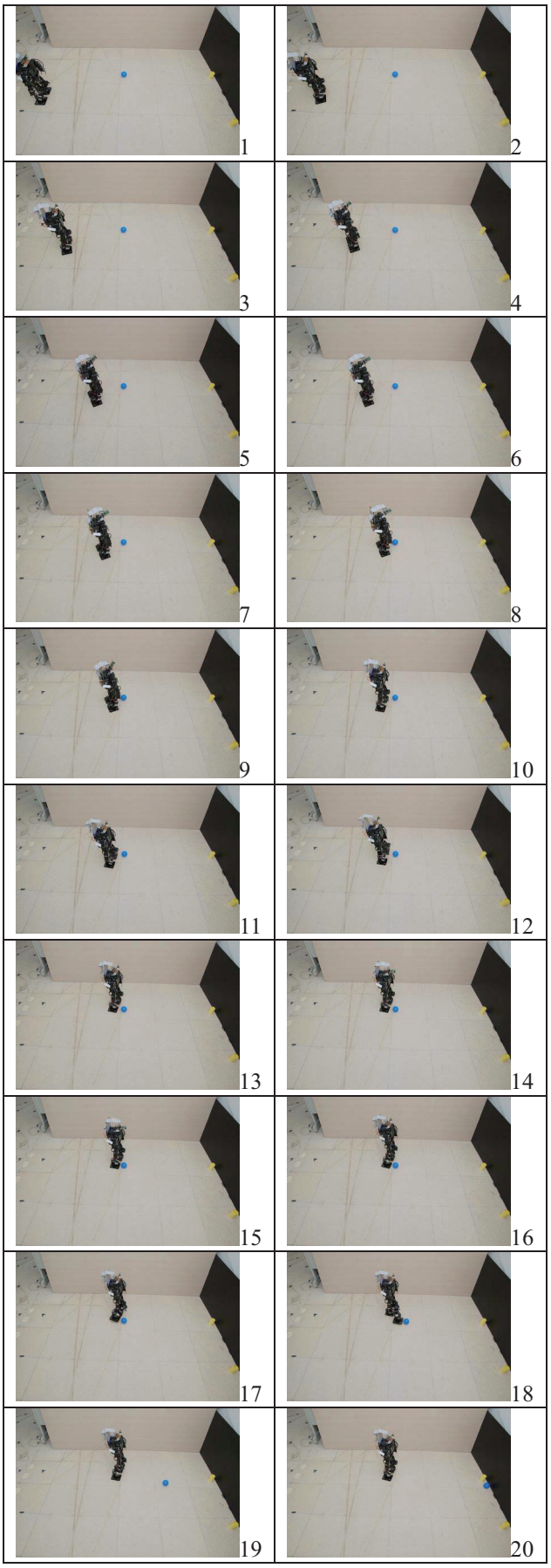

Fig. 19. Experimental result of the PK of an HR.

VII. Conclusions

The penalty kick (PK) of the soccer game for the humanoid robot is developed. The proposed system includes the following three subsystems: a humanoid robot with 22 degree-of-freedom, a soccer with different colors, and a soccer gate. For simplicity, the locations of the gate and the virtue target point are assumed to be known in advance. In addition, the initial position of the HR is in the middle line of the gate. If these conditions are not met, the AEVS also can find the gate and then initialize again for obtaining the above conditions. In the beginning, the HR scans the soccer field to find the gate and the soccer, which is randomly placed in a trapezium in the front of the gate. If a command for the PK of a specific color of soccer is assigned, the HR will be navigated by an active embedded vision system with the effective modeling via MNN and LMBP learning algorithm. After the HR reaches a neighborhood of the planned position, the search of the virtue target point is made to adjust the orientation of the HR to face it. Then the posture revision via visual navigation includes the following two steps: (i) the revision of the orientation of the HR, and (ii) the revision of the position of the HR. Finally, the smallest visual window with localization error 0.14 *cm* is employed to confirm the posture of the HR to obtain a perfect task of the PK. If not, a final fine tuning can be made to adjust its posture. The proposed experiments confirm the effective and efficiency of the AEVS via the MNN modeling and the strategy of the navigation of the HR.

References

[1] K. Loffler, M. Gienger, F. Pfeiffer and H. Ulbrich, "Sensors and control concept of a biped robot," *IEEE Trans. Ind. Electron.*, vol. 51, no. 5, pp.972-980, Oct. 2004.

[2] Q. Huang and Y. Nakamura, "Sensory reflex control for humanoid walking," *IEEE Trans. Robotics,* vol. 21, no. 5, pp. 977-984, Oct. 2005.

[3] Y. Guan, E. S. Neo, K. Yokoi and K. Tanie, "Stepping over obstacles with humanoid robots," *IEEE Trans. Robotics*, vol. 22, no. 5, pp. 958-973, Oct. 2006.

[4] K. Harada, S. Kajita, F. Kanehiro, K. Fujiwara, K. Kaneko, K. Yokoi and H. Hirukawa, "Real-time planning of humanoid robot's gait for force-controlled manipulation," *IEEE/ASME Trans. Mechatron.*, vol. 12, no. 1, pp. 53-62, Feb., 2007.

[5] E. S. Neo, K. Yokoi, S. Kajita and K. Tanie, "Whole-body motion generation integrating operator's intention and robot's autonomy in controlling humanoid robots," *IEEE Trans. Robotics*, vol. 23, no. 4, pp.763-775, Aug. 2007.

[6] D. Xu, Y. F. Li, M. Tan and Y. Shen, "A new active visual for humanoid robots," *IEEE Trans. Syst. Man & Cyber., Part B*, vol. 38, no. 2, pp. 320-330, Apr. 2008.

[7] G. Arechavaleta, J. P. Laumond, H. Hicheur, and A. Berthoz, "An optimality principle governing human walking," *IEEE Trans. Robotics*, vol. 24, no. 1, pp. 5-14, Feb. 2008.

[8] L. Montesano, M. Lopes, A. Bernardino, and Jos´e Santos-Victor, "Learning object affordances: from sensory–motor coordination to imitation," *IEEE Trans. Robotics*, vol. 24, no. 1, pp. 15-264, Feb. 2008.

[9] C. Fu and K. Chen, "Gait synthesis and sensory control of stair climbing for a humanoid robot," *IEEE Trans. Ind. Electronics,* vol. 55, no. 5, pp. 2111-2120, May 2008.

[10] T. Kanda, T. Miyashita, T. Osada, Y. Haikawa, and H. Ishiguro, "Analysis of humanoid appearances in human–robot interaction," *IEEE Trans. Robotics*, vol. 24, no. 3, pp. 725-735, Jun. 2008.

[11] E. Yoshida, C. Esteves, I. Belousov, J. P. Laumond, T. Sakaguchi and K. Yokoi, "Planning 3-D collision-free dynamic robotic motion through iterative reshaping," *IEEE Trans. Robotics*, vol. 24, no. 3, pp. 1186-1197, Oct. 2008.

[12] C. Chevallereau, J. W. Grizzle and C. L. Shih, "Asymptotically stable walking of a five-link underactuated 3-D bipedal robot", *IEEE Trans. Robotics*, vol. 25, no. 1, pp. 37-50, Feb. 2009.

[13] J. Y. Choi, B. R. So, B. J. Yi, W. Kim, and I. H. Suh, "Impact based trajectory planning of a soccer ball in a kicking robot," in Proc. Int. Conf. Robot. Autom., Barcelona, Spain, 2005, pp. 2834–2840.

[14] C.C. Wong, C.T. Cheng, K.H. Huang, Y.T. Yang, Y.Y. Hu, H.M. Chan, and H.C. Chan, "Humanoid soccer robot: TWNHR-IV", 2008 FIRA Robot World Congress.

[15] Z. Chen and M. Hemami, "Sliding mode control of kicking a soccer ball in the sagittal plane," I*EEE Trans. Syst. Man & Cybernectics, Part A*, vol. 37, no. 6, Nov. 2007.

[16] E. Menegatti, A. Pretto, A. Scarpa, and E. Pagello, "Omni-directional vision scan matching for robot localization in dynamic environments," *IEEE Trans. Robotics*, vol. 22, no. 3, pp. 523-535, Jun. 2006.

[17] K. T. Song and J. C. Tai, "Dynamic calibration of pan-tilt-zoom cameras for traffic monitoring," *IEEE Trans. Syst. Man & Cybern., Pt. B*, vol. 36, no. 5, pp. 1091-1103, Oct. 2006.

[18] I. H. Chen and S. J. Wang, "An effective approach for the calibration of multiple PTZ cameras," *IEEE Trans. Automat. Sci. & Engr.*, vol. 4, no. 2, pp. 286-293, Apr. 2007.

[19] P. Vadakkepat, P. Lim, L. C. De Silva, L. Jing and L. L. Ling, "Multimodal approach to human-face detection and tracking," *IEEE Trans. Ind. Electron.,* vol. 55, no. 3, pp. 1385-1393, Mar. 2008.